Int J Clin Exp Med 2018;11(11):11876-11888
www.ijcem.com /ISSN:1940-5901/IJCEM0081143

Original Article

DNA methylation profiles in the hippocampus of an Alzheimer's disease mouse model at mid-stage neurodegeneration

Xiaoqin Tang[1*], Sibei Ruan[1*], Qiongyao Tang[2], Juan Huang[1], Xia Luo[1,3], Xin Li[1], Siyi Luo[1], Ziqing Gao[1], Qingmei Kang[1], Yaping Tang[4,5], Mingxi Tang[1]

[1]Department of Pathology, The Affiliated Hospital of Southwest Medical University, Luzhou 646000, Sichuan, China; [2]Jiangsu Province Key Laboratory of Anesthesiology, Xuzhou Medical University, Xuzhou 221000, Jiangsu, China; [3]The Medical Department of Guizhou Province Bijie First Municipal People's Hospital, Bijie 551700, Guizhou, China; [4]Department of Neuroscience, The Southwest Medical University, Luzhou 646000, Sichuan, China; [5]Neurogenesis and Behavioral Genetics Laboratory, Guangzhou Institute of Pediatrics, Guangzhou Women and Children's Medical Center, Guangzhou 510000, Guangdong, China. [*]Equal contributors.

Received April 17, 2018; Accepted October 26, 2018; Epub November 15, 2018; Published November 30, 2018

Abstract: Aberrant DNA methylation is involved in many neurodegenerative diseases, such as Alzheimer's disease (AD), and at the same time, the hippocampus is one of the most vulnerable brain regions to AD. However, the methylation profiles in the hippocampus in a specific disease stage is hard to be determined in patients. Our previous work has demonstrated that double knockout of presenilin-1 (*PS1*) in the forebrain and presenilin-2 (*PS2*) in the mouse (dKO) could model some aspects of AD, including age-dependent neurodegeneration and massive neuronal loss at the late stage. Here, we employed reduced representation bisulfite sequencing (RRBS), together with analytical tools including Bismarkbisulfite mapper (v0.7.4), NGSQCToolkit_v2.3 software and Visualization and Integrated Discovery (DAVID) v6.8, to compare the difference in DNA methylation profiles in the hippocampus between dKO mice and their wild-type littermates at the middle stage neurodegeneration (12 months old). The results revealed that 2770 CpG sites existed in dKO mice, representing 2172 genes, might be theoretically related to neurodegeneration. Among those genes, we identified 126 genes that were abnormally methylated in the hippocampus of dKO mice, compared to those in the same brain region of wild-type mice. These genes were mainly involved in the PI3K/Akt and focal adhesion signaling pathway. Our results provide the first line of evidence showing that specific pattern of abnormal DNA methylation in the hippocampus is associated with the AD-like neurodegeneration at the middle stage disease, and furthering our understanding on how aberrant DNA methylation is involved in AD pathology.

Keywords: DNA methylation, Alzheimer's disease (AD), presenilin-1, conditional knockout, mice

Introduction

Dementia is a clinical syndrome that is featured by difficulties in language, severe deficits in cognitive function including learning and memory, mental disabilities, and disruption of activities in daily life [1]. A report from 2016 World Alzheimer conference indicates that there were 47 million people living with dementia worldwidely, and this number will climb up to 74.7 million in 2030, and 131.5 million in 2050 [2]. As one of the most common types of dementia, Alzheimer's disease (AD) is characterized by a progressive decline in cognitive and executive functions, in which the earliest clinical symptom in deficit in learning and memory. In correspondently, the pathological changes, especially synapse loss and neuronal degeneration occur at the first in the hippocampus [3-5]. Moreover, senile plaques and neurofibrillary tangles (NFTs) are also typical pathological features. Senile plaques are mainly composed of β-amyloid (Aβ), while NFTs are aggregates of hyperphosphorylated microtubule-associated tau protein [4-6]. Currently, the pathogenesis of AD is still far from clear, but recent evidence has suggested that epigenetic changes may play a critical role [7].

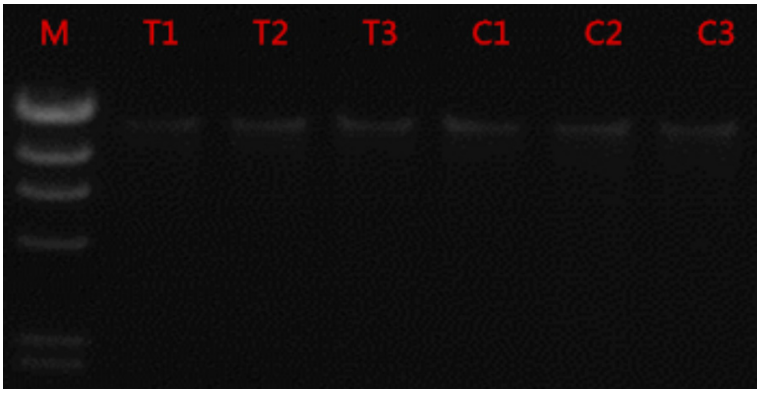

Figure 1. Hippocampal DNA samples electrophoresed on a 0.8% agarose gel. M = DNA marker, T = test samples of dKO mice, and C = control samples of wild-type mice.

In 1942, Conrad Waddington first proposed the concept of epigenetics, which is defined by the changes in gene expression without affecting the DNA nucleotide sequence. These changes include DNA methylation and hydroxymethylation, histone modifications, and non-coding RNA regulation [6, 8]. DNA methylation (5-methylcytosine [5mC]), which is a fundamental epigenetic mechanism, is achieved by a family of enzymes called DNA methyltransferases that catalyze transferring a methyl group from the methyl group donor S-adenosyl-L-methionine to the fifth carbon of cytosine residues. Methylation in the human genome occurs predominantly on CpG motifs, most of which are found in clusters (CpG islands). They are enriched in promoter regions of many genes, where methylation often leads to gene transcription silencing [8, 9]. Recent reports have indicated that epigenetic alterations may play an important role in pathogenesis of AD, while few studies have been undertaken on a genome-wide scale to distinguish latent genes/sites involved in the disease [10]. Here, we report DNA methylation profiles in the hippocampus of presenilin-1 (*PS1*)/presenilin-2 (*PS2*) conditional double knockout (dKO) mice that show AD-like neurodegeneration since 7-10 months in age (early stage) together with impairment in learning and memory, progress into significant neuronal loss at the middle stage (11-14 months old), and massive neuronal loss and dementia-like phenotype at the late stage (15-18 months old). Our results provide insight into the epigenetic mechanism underlying aging-dependent neurodegeneration.

Materials and methods

Mouse genotypes

Parental dKO mice were obtained from Professor Ya-Ping Tang (Louisiana State University, New Orleans, USA), and the genetic background of these mice was B6/CBA. Production and genotyping of dKO mice (*fPS1/fPS1; PS2-/-; Cre+/-*) have been described previously [4, 11, 12]. Genotyping was determined by PCR analyses of tail genomic DNA. Since dKO mice harbored a hemizygous allele (*Cre* transgene) and 2 homozygous alleles (*PS1* floxed and *PS2* knockout), it was impossible to obtain true wild-type mice as controls from the littermates of dKO mice [4, 12]. Therefore, we used 3 wild-type mice (in the C57BL6/CBA hybrid background) as controls. All these mice were male, in order to avoid any potential effect from estrogen cycles, and were at the age of 12 months old. All studies in animals were conducted in accordance with the Guidelines for Experimental Animals from the Ministry of Science and Technology (Sichuan, China). This study was approved by the Ethics Committee of the Southwest Medical University of China, Luzhou, Sichuan, China (LY201310).

DNA extraction from the hippocampus

Six mice were killed by decapitation. Within 1 min, the brains were dissected out. Blood was rinsed off with precooled ultrapure PBS, and the cortex, hippocampus, and cerebellum were separated quickly, frozen immediately in liquid nitrogen, and then stored at -80°C. The cerebellum used here was considered as an internal (brain region) control, since the neurodegeneration was not observed at this brain region. The genomic DNA was isolated from the hippocampus using a TIANamp Genomic DNA Kit (DP304, Tiangen, Beijing, China), according to the manufacturer's instructions. Concentration and purity of DNA were determined by OD260: 280 (OD260: 280 ≥ 1.8) and OD260: 230 (OD260: 230 ≥ 1.5), respectively, using a NanoDrop ND-1000 spectrophotometer (Nanodrop Technologies, Wilmington, DE, USA). DNA samples were stored at -20°C until used.

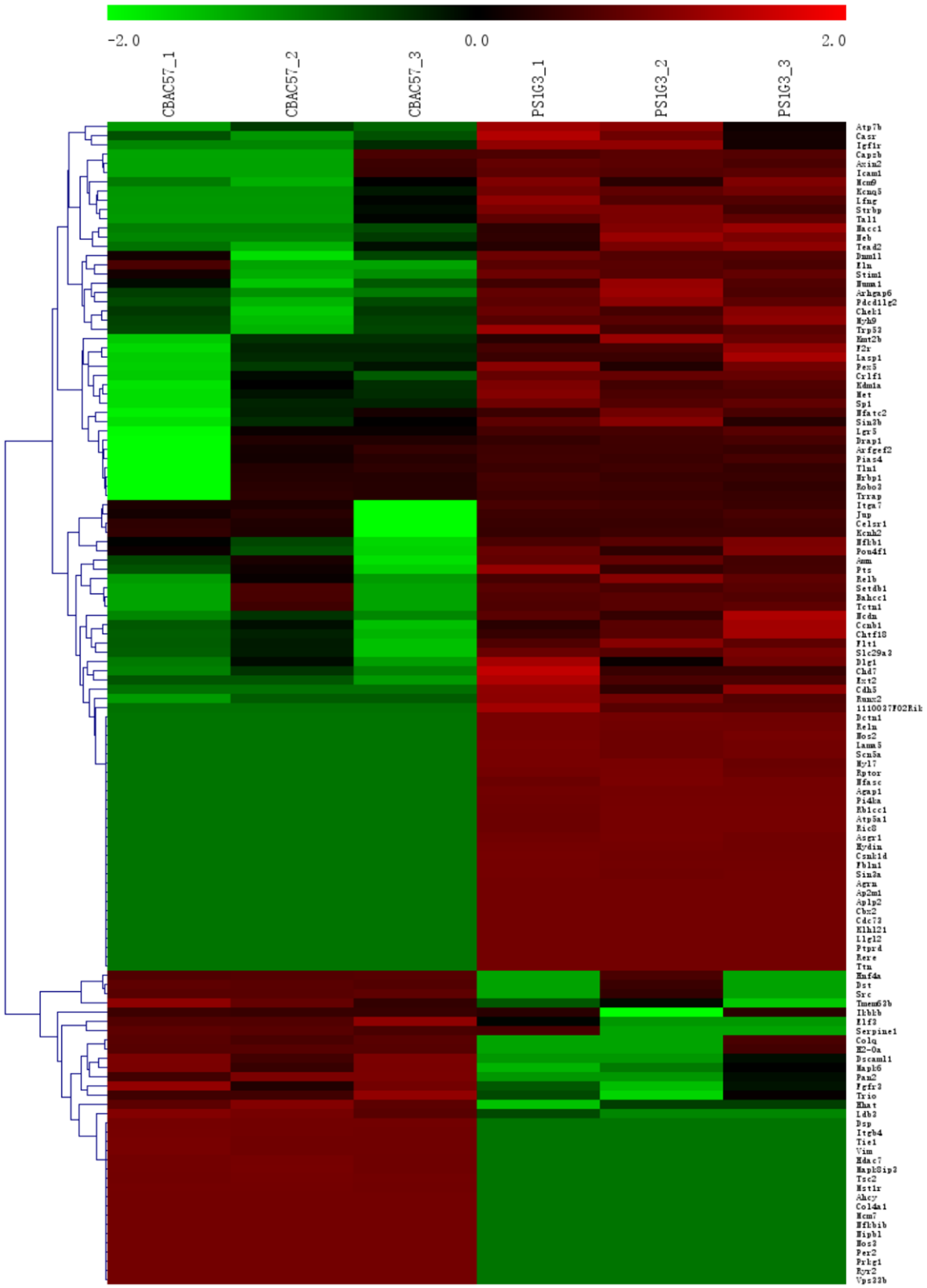

Figure 2. Hierarchical clustering of genes that showed differential expression in dKO and wild-type mice. Red and green colors indicate high and low levels of DNA methylation, respectively.

Table 1. The top 25 CpG sites located in promoter or exon regions with different methylation in dKO mice

Chr	Start	End	*P*-value	Methylation	Annotation Element	Gene Symbol
Chr1	143691414	143691477	1.11E-16	Hypomethylation	Exon	*CDC73*
Chr15	8336854	8336958	1.11E-16	Hypermethylation	Exon	*NIPBL*
Chr1	91432808	91432893	1.11E-16	Hypermethylation	Exon	*PER2*
Chr13	11741854	11742081	1.11E-16	Hypermethylation	Exon	*RYR2*
Chr1	89887506	89887762	3.12E-08	Hypermethylation	Exon	*AGAP1*
Chr16	20541956	20542092	3.12E-08	Hypomethylation	Exon	*AP2M1*
Chr11	119023258	119023302	3.12E-08	Hypomethylation	Exon	*CBX2*
Chr8	11241122	11241209	3.12E-08	Hypermethylation	Exon	*COL4A1*
Chr4	152014307	152014380	3.12E-08	Hypomethylation	Exon	*KLHL21*
Chr11	115855063	115855106	3.12E-08	Hypomethylation	Exon	*LLGL2*
Chr2	52238192	52238300	3.12E-08	Hypermethylation	Exon	*NEB*
Chr5	24372634	24372739	3.12E-08	Hypermethylation	Exon	*NOS3*
Chr19	31302286	31302400	3.12E-08	Hypermethylation	Exon	*PRKG1*
Chr4	76140514	76140703	3.12E-08	Hypomethylation	Exon	*PTPRD*
Chr4	150618406	150618553	3.12E-08	Hypomethylation	Exon	*RERE*
Chr2	76841768	76841837	3.12E-08	Hypomethylation	Exon	*TTN*
Chr7	80283980	80284077	3.12E-08	Hypermethylation	Exon	*VPS33B*
Chr9	31151837	31151993	3.12E-08	Hypomethylation	Exon	*APLP2*
Chr14	34567398	34567568	0.000902	Hypermethylation	Exon	*LDB3*
Chr2	157469125	157469279	0.001056	Hypermethylation	Exon	*SRC*
Chr11	119022829	119023529	0.001737	Hypomethylation	Promoter	*CBX2*
Chr1	21961181	21961943	0.001921	Hypomethylation	Exon	*KCNQ5*
Chr9	21025544	21025859	0.001924	Hypomethylation	Exon	*ICAM1*
Chr15	85244183	85244307	0.002058	Hypomethylation	Exon	*FBLN1*
Chr17	44724745	44724902	0.002279	Hypomethylation	Exon	*RUNX2*

Genotype was determined by using PCR amplification of genomic DNA extracted from tails of mice.

Reduced representation bisulfite sequencing (RRBS) library construction

RRBS libraries [13] were prepared according to Illumina's protocols and sequenced (IlluminaGAIIx, Illumina, San Diego, CA, USA). Briefly, genomic DNA was digested with a restriction endonuclease. The restriction fragments were then size-selected to 40-220 bp, and an adapter was ligated after size selection. The DNA was denatured, and unmethylated cytosines were bisulfite-converted to uracil. Specific primers for the modified adapter sequence [14] were used for PCR amplification, and PCR products were cloned and sequenced [14]. Then we used an application, NGSQCToolkit_v2.3 software (http://www.nipgr.res.in/ngsqctoolkit.html), for quality control of the sequence data and filtering high-quality sequence data.

Data analyses

After sequencing, we used Bismark bisulfite mapper (v0.7.4) (http://www.bioinformatics.babraham.ac.uk/projects/bismark/) and Pearson's χ^2 text to compare with GRCm38/mm10, to map bisulfite-converted sequence reads and determine cytosine methylation states. Then differentially methylated genes were screened out, and cluster analyzed using TM4 software (http://www.tm4.org/). $P < 0.05$ was regarded as statistically significant. To analyze the biological annotation terms and pathways from these target genes, the Database for Annotation, Visualization and Integrated Discovery (DAVID) Bioinformatics Resources v6.8 (http://david.abcc.ncifcrf.gov/) [15], a comprehensive set of functional annotation tools, was employed for the Gene ontology (GO) analy-

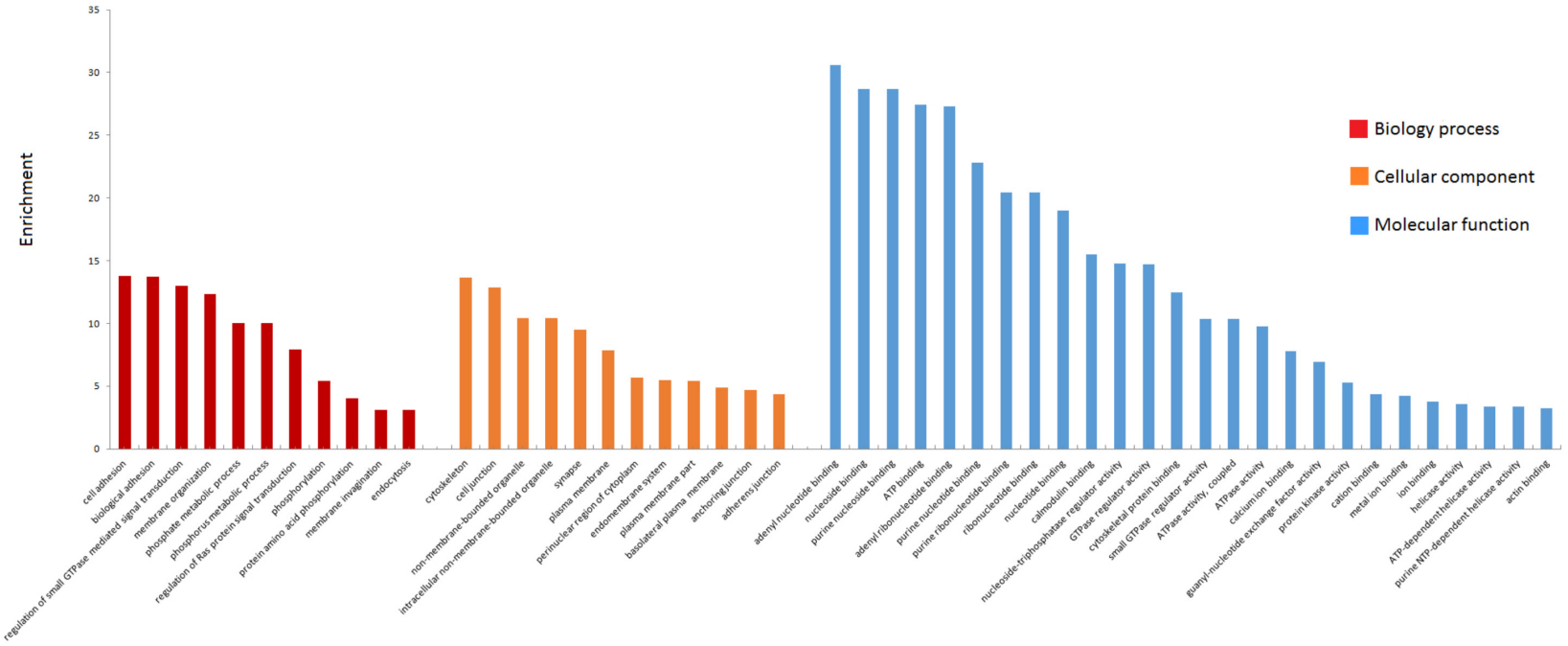

Figure 3. Significant GO categories identified by the functional annotation tool DAVID. Red, orange and blue colors indicate biological processes, cellular components and molecular functions of GO enrichment, respectively.

Table 2. Top five biological processes of abnormally methylated genes ranked by statistical significance

Term	Enriched Genes	FDR	*P*-value
GO:0007155~ cell adhesion	*ARHGAP6, CDH5, CELSR1, TLN1, DLG1, DSCAML1, DST, ICAM1, ITGA7, ITGB4, JUP, LAMA5, MYH9, NFASC, RELN, SRC*	1.00E-06	5.51E-10
GO:0022610~ biological adhesion	*ARHGAP6, CDH5, CELSR1, TLN1, DLG1, DSCAML1, DST, ICAM1, ITGA7, ITGB4, JUP, LAMA5, MYH9, NFASC, RELN, SRC*	1.11E-06	6.11E-10
GO:0051056~ regulation of small GTPase mediated signal transduction	*AGAP1, ARFGEF2, RELN, TRIO, TSC2, TTN*	2.27E-06	1.25E-09
GO:0016044~ membrane organization	*AGRN, ASGR1, DLG1, PEX5, TIE1, TRP53*	4.53E-06	2.49E-09
GO:0006796~ phosphate metabolic process	*ATP5A1, CCNB1, CHEK1, CSNK1D, F2R, FGFR3, FLT1, IGF1R, IKBKB, MAPK6, MAPK8IP3, MET, MST1R, NRBP1, PI4KA, PRKG1, PTPRD, RELN, SRC, TIE1, TRIO, TTN*	4.39E-05	2.41E-08

Table 3. Top five cellular components of abnormally methylated genes ranked by statistical significance

Term	Enriched Genes	FDR	*P*-value
GO:0005856~ cytoskeleton	*ARHGAP6, CAPZB, CCNB1, CHEK1, DCTN1, DLG1, DST, LASP1, LDB3, MST1R, MYH9, MYL7, NEB, NOS2, NOS3, NUMA1, STRBP, TLN1, TTN, VIM*	1.19E-06	8.16E-10
GO:0030054~ cell junction	*CAPZB, CDH5, COLQ, DLG1, DSP, DST, JUP, LASP1, MYH9, SCN5A, TLN1*	2.52E-06	1.73E-09
GO:0043228~ non-membrane-bounded organelle	*ARHGAP6, CAPZB, CBX2, CCNB1, CHD7, CHEK1, DCTN1, DLG1, DST, JUP, LASP1, LDB3, MST1R, MYH9, MYL7, NEB, NOS2, NOS3, NUMA1, SETDB1, SIN3A, SIN3B, STRBP, TLN1, TRP53, TTN, VIM*	3.02E-05	2.08E-08
GO:0043232~ intracellular non-membrane-bounded organelle	*ARHGAP6, CAPZB, CBX2, CCNB1, CHD7, CHEK1, DCTN1, DLG1, DST, JUP, LASP1, LDB3, MST1R, MYH9, MYL7, NOS2, NOS3, NUMA1, SETDB1, SIN3A, SIN3B, STRBP, TLN1, TRP53, TTN, VIM*	3.02E-05	2.08E-08
GO:0045202~ synapse	*AGRN, COLQ, DLG1, F2R, MYH9*	7.26E-05	4.99E-08

sis and Kyoto Encyclopedia of Genes and Genomes (KEGG) enrichment analysis. The enriched GO terms and enriched KEGG pathways were determined by the *P*-values calculated by modified Fisher Exact test. Both $P < 0.05$ and FDR (false discovery rate) < 0.05 were reported.

Results

DNA quality

DNA was extracted from the hippocampus of 3 male dKO mice at 12 months of age and 3 age- and gender-matched control mice. The bands in agarose gel electrophoresis were unbroken and clear with no obvious diffusion or trailing (**Figure 1**). The results of DNA analysis with an ultraviolet spectrophotometer showed that concentration (100~140 ng/μL) and purity (A260/A280: 1.97~2.04) were acceptable.

Distribution and pattern of DNA methylation

As described above, the distribution and pattern of DNA methylation were determined with RRBS. In total there were 2770 aberrant methylated sites (1094 hypermethylated sites and 1676 hypomethylated sites) that distributed on different chromosomes and were identified, involving 2172 target genes ($P < 0.05$). Among them, 23.75%, 19.93%, 49.24%, 7.08% were located in promoter, exon, intron, and intergenic regions, respectively. In addition, we filtered 126 genes that were differentially methylated. They were significantly different with case status and were depicted in a heat map (**Figure 2**) using TM4 software. The top 25 CpG sites,

Table 4. Top five molecular functions of abnormally methylated genes ranked by statistical significance

Term	Enriched Genes	FDR	*P*-value
GO:0030554~ adenyl nucleotide binding	*ATP5A1, ATP7B, CHD7, CHEK1, CHTF18, CSNK1D, DSCAML1, FGFR3, FLT1, IGF1R, IKBKB, KDM1A, MAPK6, MCM7, MCM9, MET, MST1R, MYH9, NOS2, NOS3, NRBP1, PRKG1, RUNX2, SRC, TIE1, TRIO, TRP53, TTN*	5.35E-14	3.33E-17
GO:0001882~ nucleoside binding	*ATP5A1, ATP7B, CHD7, CHEK1, CHTF18, CSNK1D, DSCAML1, FGFR3, FLT1, IGF1R, IKBKB, KDM1A, MAPK6, MCM7, MCM9, MET, MST1R, MYH9, NOS2, NOS3, NRBP1, PRKG1, RUNX2, SRC, TIE1, TRIO, TTN*	3.55E-13	1.69E-16
GO:0001883~ purine nucleoside binding	*ATP5A1, ATP7B, CHD7, CHEK1, CHTF18, CSNK1D, DSCAML1, FGFR3, FLT1, IGF1R, IKBKB, KDM1A, MAPK6, MCM7, MCM9, MET, MST1R, MYH9, NOS2, NOS3, NRBP1, PRKG1, RUNX2, SRC, TIE1, TRIO, TRP53, TTN*	3.55E-13	2.07E-16
GO:0005524~ ATP binding	*ATP5A1, ATP7B, CHD7, CHEK1, CHTF18, CSNK1D, DSCAML1, FGFR3, FLT1, IGF1R, IKBKB, MAPK6, MCM7, MCM9, MET, MST1R, MYH9, NRBP1, PRKG1, RUNX2, SRC, TIE1, TRIO, TRP53, TTN*	1.24E-12	8.27E-16
GO:0032559~ adenyl ribonucleotide binding	*ATP5A1, ATP7B, CHD7, CHEK1, CHTF18, CSNK1D, DSCAML1, FGFR3, FLT1, IGF1R, IKBKB, MAPK6, MCM7, MCM9, MET, MST1R, MYH9, NRBP1, PRKG1, RUNX2, SRC, TIE1, TRIO, TRP53, TTN*	1.42E-12	8.52E-16

located in promoter or exon regions, which were significantly differentially methylated in dKO mice are shown in **Table 1**.

GO and KEGG analysis

There were 3 domains of gene product properties in GO enrichment (**Figure 3**). The significant biological processes based on 43 genes mainly included cell adhesion, biological adhesion, metabolic processes, membrane organization, and signal transduction. The cellular components based on 66 genes mainly included the cytoskeleton, cell junctions, organelles, and synapses. The molecular functions based on 61 genes included nucleotide binding, enzyme activity, and ion binding. **Table 2** shows the top five biological processes, **Table 3** shows the top five cellular components, and **Table 4** shows the top five molecular functions of abnormally methylated genes ranked by statistical significance ($P < 0.05$, FDR < 0.05) in dKO mice, respectively. KEGG pathway mapping of these genes revealed that they were enriched in phosphatidylinositol 3-kinase (PI3K)/protein kinase B (AKT) signaling and focal adhesion signaling pathway. The subnetworks were composed of 14 focus genes in the PI3K/Akt signaling pathway (**Figure 4**, marked with stars) and 11 focus genes in focal adhesion signaling pathway (**Figure 5**, marked with stars). The focus genes for PI3K/Akt signaling pathway included *FLT1, COL4A1, MET, ITGB4, NFKB1, RPTOR, IGF1R, LAMA5, ITGA7, TSC2, NOS3, RELN, IKBKB* and *F2R* (**Figure 4**). The focus genes for focal adhesion signaling pathway included *IGF1R, MYL7, TLN1, FLT1, COL4A1, LAMA5, MET, ITGA7, ITGB4, RELN* and *SRC* (**Figure 5**).

Discussion

Depending on age of onset, AD can be divided into early-onset AD (EOAD) and late-onset AD (LOAD) [9]. EOAD is rare (~2% of AD cases) and occurs before the age of 65. It is primarily caused by uncommon variants in the amyloid precursor protein (*APP*), presenilin-1 (*PS1*), or presenilin-2 (*PS2*) genes [4, 8]. As polytopic membrane proteins, PS1 and PS2 show high homology (~60%) in amino acid sequence [11, 16]. They encompass the catalytic component of γ-secretase, which plays a critical role in intramembranous processing of APP, leading to production of Aβ peptides [17]. According to the amyloid hypothesis, Aβ peptides and their polymerides cause dementia and neurodegeneration in AD. Excessive production and accumulation of Aβ can lead to progressive damage of neuronal axons, death of neurons, and eventually AD. The mechanisms involve an imbalance in calcium homeostasis, which makes cells more vulnerable to toxic or harmful substances that can lead to further impairment and NFTs

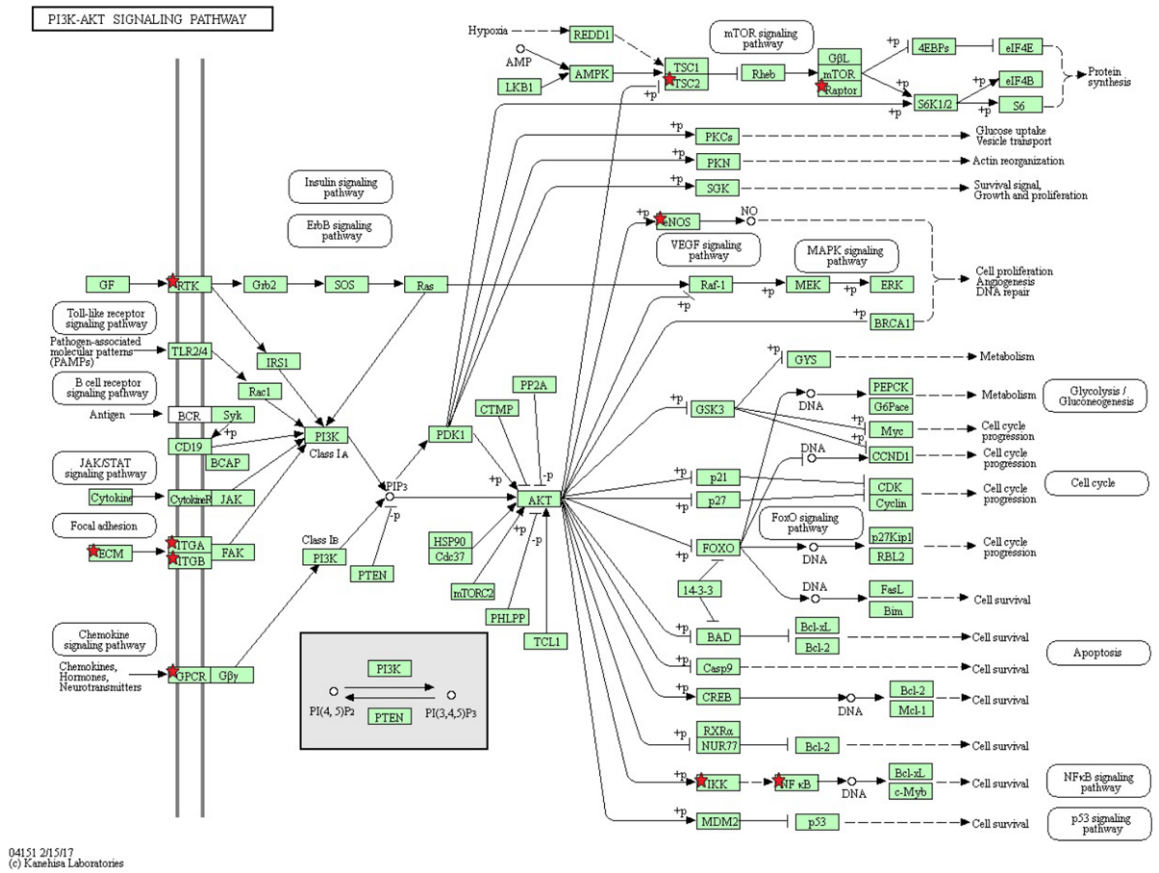

Figure 4. Differentially methylated genes in PI3K/Akt signaling pathway. Stars indicate the focus genes in PI3K/Akt signaling pathway, include *FLT1*, *COL4A1*, *MET*, *ITGB4*, *NFKB1*, *RPTOR*, *IGF1R*, *LAMA5*, *ITGA7*, *TSC2*, *NOS3*, *RELN*, *IKBKB* and *F2R*.

[6]. In contrast, LOAD is the most common form of AD and occurs mainly in the elderly over the age of 65. It is much more complicated and accounts for greater than 90% of AD cases [9, 18]. A large-scale genome-wide association study has confirmed that aberrant methylation of many genes, such as transmembrane protein 59 (*TMEM59*) [10], sortilin-related receptor 1 (*SORL1*) [19], and brain-derived nerve growth factor (*BDNF*) [3], is genetically associated with LOAD. Therefore, it is essential to establish genome-wide DNA methylation profiles of AD.

By applying a conditional genetic strategy, we used viable dKO mice in which *PS1* was conditionally deleted in the forebrain regions and *PS2* was conventionally deleted in the whole body. Because presenilins are widely expressed in the brain, and play essential roles in maintaining the neural progenitor population, neurogenesis, and neuronal migration during embryonic development [20], knockout of *PS1* at the first ontogenesis results in premature death of null mutant mice, and *PS2* can partially compensate for the function of *PS1* [4]. To fulfill the requirement for presenilins in development, the *Cre/loxP* recombinant system was used for producing conditional *PS1*-knockout mice [4, 11, 12, 20]. In dKO mice at 2 months of age, which underwent PS1 inactivation a month later, mild memory impairment, as well as specific presynaptic and postsynaptic defects were found, although there was no significant loss of cortical neurons or anatomical change [16, 20]. By 6 months of age, anatomical abnormalities developed, and gradual thinning of cortical layers became more apparent over time [16]. At 7 and 9 months of age, 18% and 24% of cortical neurons were lost, respectively. The cortical volume was reduced by 35% and lateral ventricle began to expand [4, 12]. At 12 months, all these changes, involving cortical/hippocampal

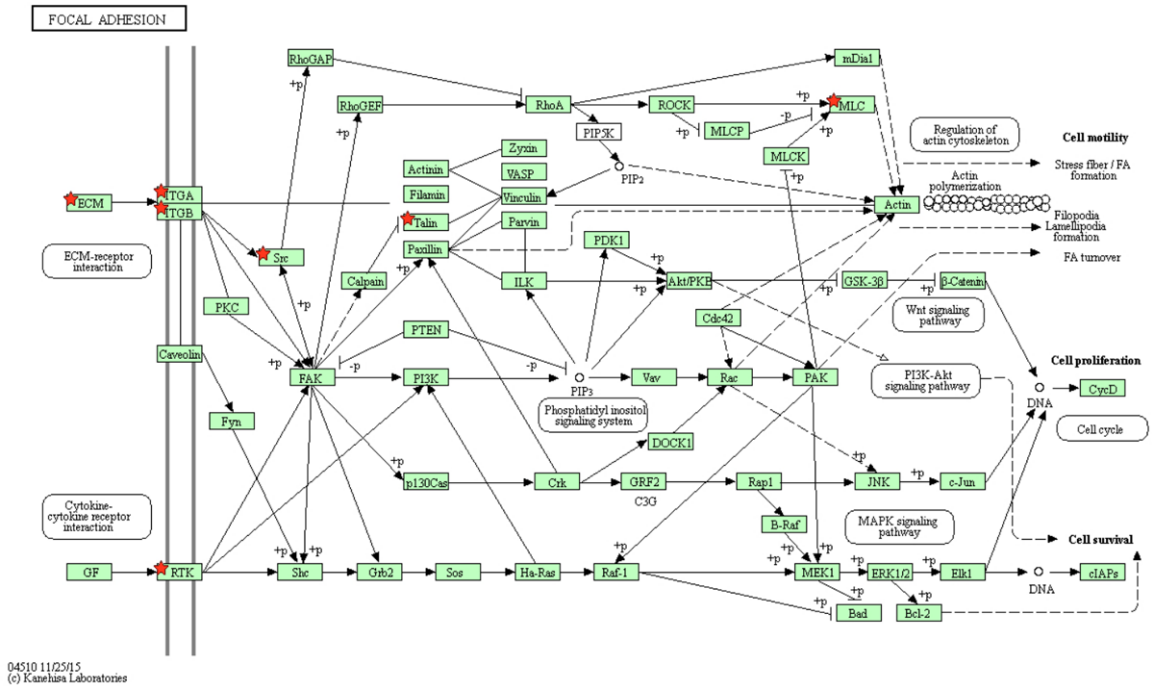

Figure 5. Differentially methylated genes in focal adhesion signaling pathway. Stars indicate the focus genes in focal adhesion signaling pathway, include *IGF1R*, *MYL7*, *TLN1*, *FLT1*, *COL4A1*, *LAMA5*, *MET*, *ITGA7*, *ITGB4*, *RELN* and *SRC*.

atrophy and enlarged lateral/third ventricles, were more serious [4]. Therefore, we believe that neurodegeneration in the knockout mice represents an AD-like neurodegeneration [12], which can be used to study pathogenic mechanisms of AD. However, this model is not a comprehensive AD model because there is no Aβ deposition in the brain [4, 12].

Analysis revealed 2770 CpG sites in dKO mice, representing 2172 unique genes potentially associated with AD. In addition, 126 genes with differentially methylated regions were screened. Among those, many of them have been demonstrated to have a link with AD. For example, AD patients have higher levels of copper and free copper than healthy controls, due to genetic variations in the copper transporter gene, *ATP7B* [21]. A member of the catenin family encoded by the *JUP* gene, is expressed at high levels in the adult and aging brain, which is characterized by a high degree of folding and firm lamination [22]. RB1-inducible Coiled-Coil 1 (*RB1CC1*) insufficiency may result in neuronal atrophy [23]. The *RELN* gene encodes Reelin, which is a serine protease and part of the apolipoprotein E (APOE) biochemical pathway [24]. Lack of NO synthase 2 (NOS2) in APP increases insoluble Aβ peptide levels, neuronal degeneration, caspase-3 activation, and tau cleavage [25]. The transcription factor encoded by the *SP1* gene partly locates on hyperphosphorylated tau deposits in NFTs and dystrophic neurites of senile plaques [26]. Deleting insulin-like growth factor 1 receptor (*IGF1R*) gene in neurons of the ageing brain genetically can efficiently protect from neuroinflammation, memory disorder and anxiety induced by intracerebroventricular injection of Aβ oligomers [27]. In the brain, *SERPINE1* encodes plasminogen activator inhibitor type-1, which regulates plasmin activation negatively and results in Aβ accumulation [28]. Finally, it is known that systemic calcium homeostasis is transformed in AD patients. The *CASR* gene encodes a G-protein coupled transmembrane receptor, which plays a role in calcium regulation. Abnormal regulation of calcium promotes susceptibility to neuronal cell damage [29]. Furthermore, a ryanodine receptor encoded by the *RyR2* gene, can give rise to several alternatively spliced messenger RNAs. These variants produce functionally distinct RyR channels that may differ in Ca^{2+} release properties or subcel-

lular localization [30]. In our study, the methylation of these genes had been changed. Thus, it can be seen that abnormal methylation of these genes may be involved in pathogenesis of AD.

Some abnormal methylated genes in dKO mice, such as amyloid precursor-like protein 2 (*APLP2*) [31] and intercellular adhesion molecule 1 (*ICAM1*) [32], have been reported to have no relevance to development of AD. In addition, research on the *NOS3* gene is controversial. Meta-analysis suggests that the *NOS3* Glu298Asp gene polymorphism is not associated with AD [33]. However, another study shows that it might be a risk factor for LOAD and dependent on *APOE* epsilon 4 status in the Chinese population [34]. In our study, they were hypomethylated and located in exon regions. Therefore, more studies are required to evaluate further the relationship between DNA methylation of these genes and AD risk.

In our study, we completed integrated analysis of CpG methylation to examine the global epigenetic abnormality from age- and gender-matched dKO mice and controls. Some changes of DNA methylation observed in this study were consistent with previous reports. For example, the promoter regions of *CPNE9* and *RELB* [10] were hypomethylated both in *APP/PS1* transgenic mice and dKO mice. It is suggested that abnormal methylation of these genes may be closely related to pathogenesis of AD, which may be candidate target genes for AD. Some of the results were not the same with previous reports. For example, hypermethylated *NR4A1* [35] was located in promoter region in *APP/PS1* transgenic mice but located in exon region in dKO mice. The promoter region of *SLC7A3* [10] was hypermethylated in human frontal cortex of LOAD but hypomethylated in our study. In *APP/PS1* transgenic mice, *PRNP* and *NOS2* [35] were hypermethylated and located in promoter regions, but they were hypomethylated and located in exon regions in dKO mice. In AD patients, *OPRD1* [36] was hypermethylated and located in promoter region, but hypomethylated and located in exon region in our study. Besides, DNA abnormal methylation in promoter CpGs of AD-associated genes such as *TGFB1* (hypermethylated) [35], *COASY* (hypermethylated) [37], *SPINT1* (hypermethylated) [37], *CTIF* and *NXT2* (hypomethylated) [38], were not observed in the genome-wide analysis of the dKO mice and controls. It may be related to the pathological stage, specimen screening, check point and different animal models. And more studies are demanded to verify the methylation of these genes in AD.

In addition, to determine whether these candidate genes with differential methylation in regard to AD pathology were linked with neurologic pathways, we accomplished GO and KEGG analysis using DAVID. The GO analysis showed these abnormal methylated genes involved in many biological processes, cellular components and molecular functions that were correlated with AD development. For example, as adhesion molecules, *CELSR1* [39] plays crucial roles in axon guidance and neuronal migration. And *DSCAML1* [40] involves in neurogenesis, axonal outgrowth, synaptogenesis, and synaptic plasticity. Moreover, some molecular functions associated with hypermethylation in dKO mice, such as GTPase regulator activity and ATPase activity [10], were the same as the LOAD cases. Functional network analysis of these candidate genes revealed subnetworks composed of focus genes in the PI3K/Akt and focal adhesion signaling pathways. Karki R et al. also demonstrated the PI3K/AKT signaling pathway in AD network model [41]. Besides, Lin J et al. found the PI3K/Akt pathway might be involved in Aβ oligomer-induced neurotoxicity in SH-SY5Y cells [42]. In AD patients, focal adhesion was one of AD endophenotype-associated pathways [43]. And the mechanism of Aβ generation, which came from the endocytosis of APP, was closely concerned with disturbance in integrin-based focal adhesion signaling [44]. Therefore, the results of our study indicated that the PI3K/Akt and focal adhesion signaling pathways may be relevant to AD pathogenesis.

The etiology and pathogenesis of AD are complex and contain many genetic and environmental risk elements. The sporadic nature of AD suggests that epigenetics is closely related to pathology of the disease [6]. As a key epigenetic modification, DNA methylation may represent heritable information that is not encoded in the nucleotide sequence [14]. Therefore, it is vital to create a genome-wide DNA methylation map of AD. As one of the modern methods for studying genome-scale DNA methylation, RRBS has been developed for high-throughput analy-

sis of DNA methylation, which is based on sequencing genomic libraries using sodium bisulfite [45]. It offers an important basis for establishing genomic DNA methylation profiling maps and identifying aberrant methylated genes, as well as clues that may be used in prevention, diagnosis, and treatment of AD.

This study advances our knowledge and understanding of the methylome and improves our understanding of the basic epigenetic molecular mechanisms related to AD. These results establish genomic DNA methylation profiling in the hippocampus mid-stage in neurodegeneration and identify genes with aberrant methylation. With these results, we may develop a new strategy or identify new molecular targets for preventing, diagnosing, and curing AD at the middle stage.

Acknowledgements

This study was funded, in part by the Key Technologies R&D Program of Sichuan Province of China (14ZC0054 to YPT), the grants from the Key Project in Sichuan province department of education (16ZA0196 to MXT), the Joint Research Fund for Luzhou Science and Technology Bureau and Southwest Medical University, China (2017LZXNYD-J14 to MXT), the Funds of the NSFC (31671212) and KC-16H0230 to QY. T, and the Funds of Southwest Medical University, China (15087, 2015-PT-003 and 2016-YJ002 to MXT, 2016027 to JH).

Disclosure of conflict of interest

None.

Address correspondence to: Dr. Mingxi Tang, Department of Pathology, The Affiliated Hospital of Southwest Medical University, 25 Taiping Street, Luzhou 646000, Sichuan, China. Tel: +86 0830-3160556; Fax: +860830-3160331; E-mail: mxtang69@163.com; Yaping Tang, Department of Neuroscience, The Southwest Medical University, Luzhou 646000, Sichuan, China. E-mail: YPtang12@126.com

References

[1] Nagata T, Kobayashi N, Ishii J, Shinagawa S, Nakayama R, Shibata N, Kuerban B, Ohnuma T, Kondo K, Arai H, Yamada H, Nakayama K. Association between DNA methylation of the BDNF promoter region and clinical presentation in Alzheimer's disease. Dement Geriatr Cogn Dis Extra 2015; 5: 64-73.

[2] Alzheimer's Association. 2016 Alzheimer's disease facts and figures. Alzheimers Dement 2016; 12: 459-509.

[3] Nagata T, Kobayashi N, Ishii J, Shinagawa S, Nakayama R, Shibata N, Kuerban B, Ohnuma T, Kondo K, Arai H, Yamada H, Nakayama K. Association between DNA methylation of the bdnf promoter region and clinical presentation in Alzheimer's disease. Dement Geriatr Cogn Dis Extra 2015; 5: 64-73.

[4] Chen Q, Nakajima A, Choi SH, Xiong X, Tang YP. Loss of presenilin function causes Alzheimer's disease-like neurodegeneration in the mouse. J Neurosci Res 2008; 86: 1615-1625.

[5] Li T, Yu Y, Cai H. Effects of brain-derived neurotrophic factor-pretreated neuron stem cell transplantation on Alzheimer's disease model mice. Int J Clin Exp Med 2015; 8: 21947-21955.

[6] Adwan L, Zawia NH. Epigenetics: a novel therapeutic approach for the treatment of Alzheimer's disease. Pharmacol Ther 2013; 139: 41-50.

[7] Chouliaras L, Mastroeni D, Delvaux E, Grover A, Kenis G, Hof PR, Steinbusch HW, Coleman PD, Rutten BP, van den Hove DL. Consistent decrease in global DNA methylation and hydroxymethylation in the hippocampus of Alzheimer's disease patients. Neurobiol Aging 2013; 34: 2091-2099.

[8] Lashley T, Gami P, Valizadeh N, Li A, Revesz T, Balazs R. Alterations in global DNA methylation and hydroxymethylation are not detected in Alzheimer's disease. Neuropathol Appl Neurobiol 2015; 41: 497-506.

[9] Coppieters N, Dieriks BV, Lill C, Faull RL, Curtis MA, Dragunow M. Global changes in DNA methylation and hydroxymethylation in Alzheimer's disease human brain. Neurobiol Aging 2014; 35: 1334-1344.

[10] Bakulski KM, Dolinoy DC, Sartor MA, Paulson HL, Konen JR, Lieberman AP, Albin RL, Hu H, Rozek LS. Genome-wide DNA methylation differences between late-onset Alzheimer's disease and cognitively normal controls in human frontal cortex. J Alzheimers Dis 2012; 29: 571-588.

[11] Feng R, Wang H, Wang J, Shrom D, Zeng X, Tsien JZ. Forebrain degeneration and ventricle enlargement caused by double knockout of Alzheimer's presenilin-1 and presenilin-2. Proc Natl Acad Sci U S A 2004; 101: 8162-8167.

[12] Chen Q, Nakajima A, Choi SH, Xiong X, Sisodia SS, Tang YP. Adult neurogenesis is functionally associated with AD-like neurodegeneration. Neurobiol Dis 2008; 29: 316-326.

[13] Brant JO, Riva A, Resnick JL, Yang TP. Influence of the Prader-Willi syndrome imprinting center on the DNA methylation landscape in the mouse brain. Epigenetics 2014; 9: 1540-1556.
[14] Meissner A, Gnirke A, Bell GW, Ramsahoye B, Lander ES, Jaenisch R. Reduced representation bisulfite sequencing for comparative high-resolution DNA methylation analysis. Nucleic Acids Res 2005; 33: 5868-5877.
[15] Huang da W, Sherman BT, Lempicki RA. Bioinformatics enrichment tools: paths toward the comprehensive functional analysis of large gene lists. Nucleic Acids Res 2009; 37: 1-13.
[16] Mirnics K, Norstrom EM, Garbett K, Choi SH, Zhang X, Ebert P, Sisodia SS. Molecular signatures of neurodegeneration in the cortex of PS1/PS2 double knockout mice. Mol Neurodegener 2008; 3: 14.
[17] Xia D, Watanabe H, Wu B, Lee SH, Li Y, Tsvetkov E, Bolshakov VY, Shen J, Kelleher RJ 3rd. Presenilin-1 knockin mice reveal loss-of-function mechanism for familial Alzheimer's disease. Neuron 2015; 85: 967-981.
[18] Millan MJ. The epigenetic dimension of Alzheimer's disease: causal, consequence, or curiosity? Dialogues Clin Neurosci 2014; 16: 373-393.
[19] Wen Y, Miyashita A, Kitamura N, Tsukie T, Saito Y, Hatsuta H, Murayama S, Kakita A, Takahashi H, Akatsu H, Yamamoto T, Kosaka K, Yamaguchi H, Akazawa K, Ihara Y, Kuwano R. SORL1 is genetically associated with neuropathologically characterized late-onset Alzheimer's disease. J Alzheimers Dis 2013; 35: 387-394.
[20] Wines-Samuelson M, Schulte EC, Smith MJ, Aoki C, Liu X, Kelleher RJ 3rd, Shen J. Characterization of age-dependent and progressive cortical neuronal degeneration in presenilin conditional mutant mice. PLoS One 2010; 5: e10195.
[21] Squitti R, Polimanti R, Siotto M, Bucossi S, Ventriglia M, Mariani S, Vernieri F, Scrascia F, Trotta L, Rossini PM. ATP7B variants as modulators of copper dyshomeostasis in Alzheimer's disease. Neuromolecular Med 2013; 15: 515-522.
[22] Smith A, Bourdeau I, Wang J, Bondy CA. Expression of Catenin family members CTNNA1, CTNNA2, CTNNB1 and JUP in the primate prefrontal cortex and hippocampus. Brain Res Mol Brain Res 2005; 135: 225-231.
[23] Chano T, Okabe H, Hulette CM. RB1CC1 insufficiency causes neuronal atrophy through mTOR signaling alteration and involved in the pathology of Alzheimer's diseases. Brain Res 2007; 1168: 97-105.
[24] Seripa D, Matera MG, Franceschi M, Daniele A, Bizzarro A, Rinaldi M, Panza F, Fazio VM, Gravina C, D'Onofrio G, Solfrizzi V, Masullo C, Pilotto A. The RELN locus in Alzheimer's disease. J Alzheimers Dis 2008; 14: 335-344.
[25] Colton CA, Vitek MP, Wink DA, Xu Q, Cantillana V, Previti ML, Van Nostrand WE, Weinberg JB, Dawson H. NO synthase 2 (NOS2) deletion promotes multiple pathologies in a mouse model of Alzheimer's disease. Proc Natl Acad Sci U S A 2006; 103: 12867-12872.
[26] Santpere G, Nieto M, Puig B, Ferrer I. Abnormal Sp1 transcription factor expression in Alzheimer disease and tauopathies. Neurosci Lett 2006; 397: 30-34.
[27] George C, Gontier G, Lacube P, François JC, Holzenberger M, Aïd S. The Alzheimer's disease transcriptome mimics the neuroprotective signature of IGF-1 receptor-deficient neurons. Brain 2017; 140: 2012-2027.
[28] Kutz SM, Higgins CE, Higgins PJ. Novel combinatorial therapeutic targeting of PAI-1 (SERPINE1) gene expression in Alzheimer's disease. Mol Med Ther 2012; 1: 106.
[29] Conley YP, Mukherjee A, Kammerer C, DeKosky ST, Kamboh MI, Finegold DN, Ferrell RE. Evidence supporting a role for the calcium-sensing receptor in Alzheimer disease. Am J Med Genet B Neuropsychiatr Genet 2009; 150B: 703-709.
[30] Bruno AM, Huang JY, Bennett DA, Marr RA, Hastings ML, Stutzmann GE. Altered ryanodine receptor expression in mild cognitive impairment and Alzheimer's disease. Neurobiol Aging 2012; 33: 1001.e1-1001.e6.
[31] Midthune B, Tyan SH, Walsh JJ, Sarsoza F, Eggert S, Hof PR, Dickstein DL, Koo EH. Deletion of the amyloid precursor-like protein 2 (APLP2) does not affect hippocampal neuron morphology or function. Mol Cell Neurosci 2012; 49: 448-455.
[32] Mattila KM, Hiltunen M, Rinne JO, Mannermaa A, Röyttä M, Alafuzoff I, Laippala P, Soininen H, Lehtimäki T. Absence of association between an intercellular adhesion molecule 1 gene E469K polymorphism and Alzheimer's disease in Finnish patients. Neurosci Lett 2003; 337: 61-63.
[33] Hua Y, Zhao H, Kong Y, Lu X. Association between Alzheimer's disease and the NOS3 gene Glu298Asp polymorphism. Int J Neurosci 2014; 124: 243-251.
[34] Wang B, Tan S, Yang Z, Xie YC, Wang J, Zhou S, Li S, Zheng C, Ma X. Association between Alzheimer's disease and the NOS3 gene Glu298Asp polymorphism in Chinese. J Mol Neurosci 2008; 34: 173-176.
[35] Cong L, Jia J, Qin W, Ren Y, Sun Y. Genome-wide analysis of DNA methylation in an APP/PS1 mouse model of Alzheimer's disease. Acta Neurol Belg 2014; 114: 195-206.

[36] Ji H, Wang Y, Liu G, Chang L, Chen Z, Zhou D, Xu X, Cui W, Hong Q, Jiang L, Li J, Zhou X, Li Y, Guo Z, Zha Q, Niu Y, Weng Q, Duan S, Wang Q. Elevated OPRD1 promoter methylation in Alzheimer's disease patients. PLoS One 2017; 12: e0172335.

[37] Kobayashi N, Shinagawa S, Nagata T, Shimada K, Shibata N, Ohnuma T, Kasanuki K, Arai H, Yamada H, Nakayama K, Kondo K. Usefulness of DNA methylation levels in COASY and SPINT1 gene promoter regions as biomarkers in diagnosis of Alzheimer's disease and amnestic mild cognitive impairment. PLoS One 2016; 11: e0168816.

[38] Sung HY, Choi EN, Ahn Jo S, Oh S, Ahn JH. Amyloid protein-mediated differential DNA methylation status regulates gene expression in Alzheimer's disease model cell line. Biochem Biophys Res Commun 2011; 414: 700-705.

[39] Feng J, Han Q, Zhou L. Planar cell polarity genes, Celsr1-3, in neural development. Neurosci Bull 2012; 28: 309-315.

[40] Montesinos ML. Roles for DSCAM and DSCAML1 in central nervous system development and disease. Adv Neurobiol 2014; 8: 249-270.

[41] Karki R, Kodamullil AT, Hofmann-Apitius M. Comorbidity analysis between Alzheimer's Disease and Type 2 Diabetes Mellitus (T2DM) based on shared pathways and the role of T2DM drugs. J Alzheimers Dis 2017; 60: 721-731.

[42] Lin J, Yu J, Zhao J, Zhang K, Zheng J, Wang J, Huang C, Zhang J, Yan X, Gerwick WH, Wang Q, Cui W, He S. Fucoxanthin, a marine carotenoid, attenuates β-amyloid oligomer-induced neurotoxicity possibly via regulating the PI3K/Akt and the ERK pathways in SH-SY5Y cells. Oxid Med Cell Longev 2017; 2017: 6792543.

[43] Silver M, Janousova E, Hua X, Thompson PM, Montana G. Alzheimer's disease neuroimaging initiative. identification of gene pathways implicated in Alzheimer's disease using longitudinal imaging phenotypes with sparse regression. Neuroimage 2012; 63: 1681-1694.

[44] Kang DE, Roh SE, Woo JA, Liu T, Bu JH, Jung AR, Lim Y. The interface between cytoskeletal aberrations and mitochondrial dysfunction in Alzheimer's disease and related disorders. Exp Neurobiol 2011; 20: 67-80.

[45] Tanas AS, Kuznetsova EB, Borisova ME, Rudenko VV, Zaletayev DV, Strelnikov VV. [Reduced representation bisulfite sequencing design for assessing the methylation of human CpG islands in large samples]. Mol Biol (Mosk) 2015; 49: 689-699.